Geophysica (1986), Vol. 22, Nos 1–2, pp. 101–118
Printed in Finland

551.501.8
551.501.815
551.554

DOPPLER RADAR OBSERVATIONS OF HORIZONTAL ROLL VORTICES IN FINLAND

by

TIMO PUHAKKA and PIRKKO SAARIKIVI

University of Helsinki
Department of Meteorology
Hallituskatu 11–13
SF–00100 Helsinki 10
Finland

Abstract

A very sensitive Doppler weather radar at the University of Helsinki located on the shoreline of the Gulf of Finland was used to observe horizontal roll vortices in the planetary boundary layer. Of the nine roll-cases studied two occurred in a clear-air situation while in seven cases rolls were observed within widespread precipitation, either in rainfall or in snowfall. The frequent occurrence of rolls within precipitation was the most important new finding of this study. Roll wavelengths varied between 3 and 10 km, their aspect ratios typically between 5 and 10 (the most common value being 6) while their heights were normally equal to or less than 1 km (in one case only, 2.2 km). In all cases studied rolls existed over the land. Only in two cases could rolls also be observed over the sea but their heights, wavelengths and intensities were clearly smaller than of those observed simultaneously over the land. The small number of cases, the uncertainties especially in measurement of the heights of the roll circulations, and the lack of detailed suitable thermodynamical data made it difficult to reach any firm conclusions about the physical mechanisms responsible for the roll circulation in precipitating situations. In addition to inflection point instability, both the differences in the surface friction over land and sea and also the thermal instability may play a role. Some justification for the latter factor is provided by the obvious dependence of the aspect ratio on the sea-air temperature contrast.

1. *Introduction*

According to observations made from satellites and high-flying aircraft, parallel could bands are a common feature in and just above the planetary boundary layer (PBL) of the Earth's atmosphere (see *e.g.* KUETTNER (1959) and (1971), BROWN (1980)). More detailed observations have shown that cloud bands are caused by a helical secondary flow in the PBL, referred to here as horizontal roll vortices. Roll cases studied so far have mainly been in maritime cumulus cloud situations where cloud streets make the rolls visible. Observational data are typically obtained, in addition to those from normal radiosondes, from tower and aircraft measurements. Only in few cases have rolls been studied recently by radar methods (BERGER and DOVIAK (1979), HILDEBRAND (1980), KELLY (1982), KONRAD (1968), KROPFLI and KOHN (1978) and RABIN *et al.* (1981)).

The present study has used a single C-band Doppler radar to detect and analyse roll vortices in the PBL. In addition to two clear air cases, 7 fully cloudy situations with rolls were also observed. Three of these were rainfall cases and four snowfall cases. Both the analysis methods using a single Doppler radar and the possible reasons for roll circulations are discussed.

2. *The general structure of rolls*

Fig. 1 illustrates the three-dimensional structure and the secondary flow pattern of an idealized roll case. Typically rolls form within the PBL and are oriented roughly along the mean flow there. Only a few direct measurements of important roll parameters are available, (*e.g.* KUETTNER (1971), LE MONE (1973), KELLY (1984), BRÜMMER (1985), MÜLLER *et al.* (1985)). These, together with model simulations (*e.g.* FALLER and KAYLOR (1966), BROWN (1970)) suggest that roll wavelengths are typically more than twice their height (aspect ratios between 2 and 10), the relative magnitude of the cross-roll component, *Ur*, of the secondary circulation, is of the order of 10 % of the basic flow *Vg* at the top of the PBL, and the roll-parallel component, *Vr*, of the secondary circulation may be as large as 30 % of *Vg*. In most of the studies a moderate or strong wind in the PBL and a capping inversion were typical features of roll cases.

Both real observed rolls and those based on model simulations naturally have a much more complicated structure than depicted in our idealized model in fig. 1. As an example, fig. 2 shows kinematic properties of rolls from model simulations by BROWN (1970). As can be seen, for example, roll secondary flow is not circularly symmetrical, the maximum of its roll-parallel component does not coincide with the roll axis, etc. Fig. 1 indeed is only for defining the terms, and for show-

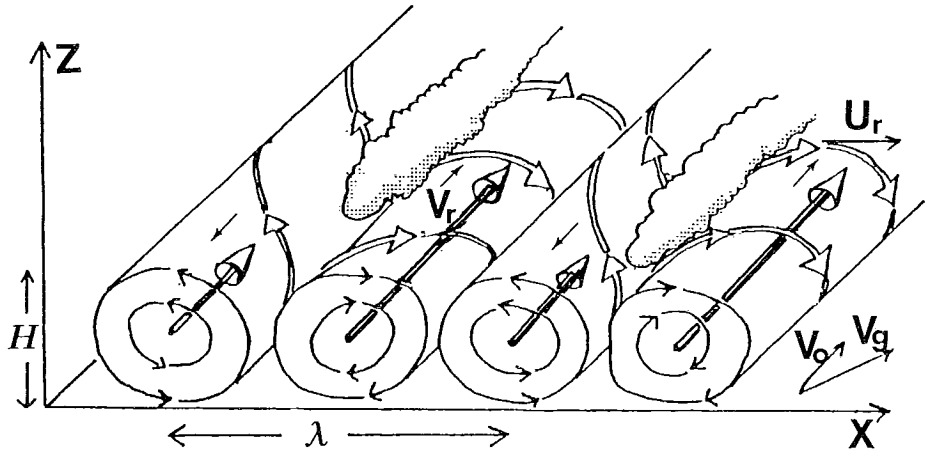

Fig. 1. Idealized secondary flow pattern of horizontal roll vortices with the definitions of some roll-parameters in a coordinate system with the y-axis parallel with the rolls. *Vg* is the wind vector (geostrophic) at the top of the PBL and *Vo* is the surface wind vector. The cross-roll component, *Ur*, and the roll-parallel component, *Vr*, of the secondary flow are also indicated.

ing those main features of rolls which could be most important in radar observations.

Many physical mechanisms have been suggested as the reason for roll formation. These include convection with suitable shear, and inflection-point instability within the PBL as the most likely basic mechanisms. Still unknown is the relative importance of these reasons in different cases, mainly because of the difficulty in obtaining accurate and detailed observational data on this size of atmospheric phenomena. For further details of the basic theory see *e.g.* KUETTNER (1971), LEMONE (1973) and (1976), BROWN (1970) and (1980), and MASON (1985).

3. *Detection of roll circulation by a Doppler radar*

In principle, both secondary flow components *Ur* and *Vr* (see fig. 1) may make roll circulations visible on a single Doppler radar PPI scan. The cross-roll component *Ur* causes alternating toward and away radial velocities in a beam pointing perpendicular to the rolls (fig. 3a). If the beam is scanning more along the direction of rolls, then still a roll-to-roll variation in the radial velocity is observed, but the differences in radial velocities decrease with decreasing angle ϕ between the beam and the rolls as the radial component, $Ur \sin\phi$, related to the cross-roll velocity,

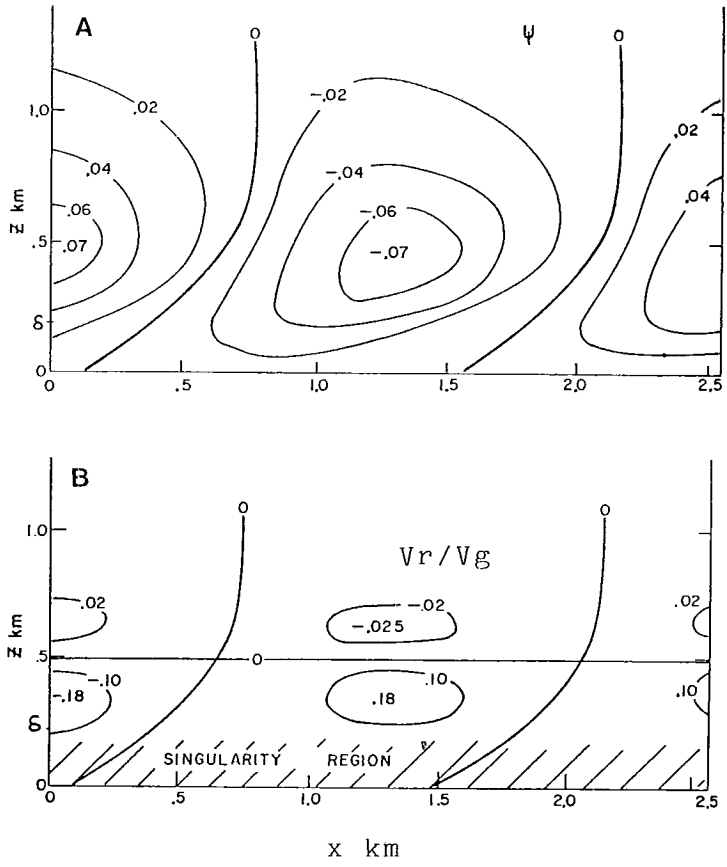

Fig. 2. An example of (a) the secondary flow stream function and (b) the secondary flow relative longitudinal component *Vr/Vg* after the secondary flow model by BROWN (1970).

approaches zero as ϕ approaches zero. However, the roll wavelength is obviously the distance (measured perpendicular to the roll direction) between two maxima (or minima) in the radial velocity everywhere, except near the roll passing through the radar location.

The contribution of the roll-parallel component *Vr* of the secondary flow to the radial velocity pattern is obvious if *Vr* is related to individual rolls as depicted in figs. 1 or 2. Figure 3b shows schematically how *Vr* contributes to roll-to-roll differences in the radial velocity; these differences are biggest for beams pointing roughly parallel with the rolls, vanishing at azimuth angles perpendicular to the rolls, just the opposite of the azimuthal dependence of the contribution of *Ur*.

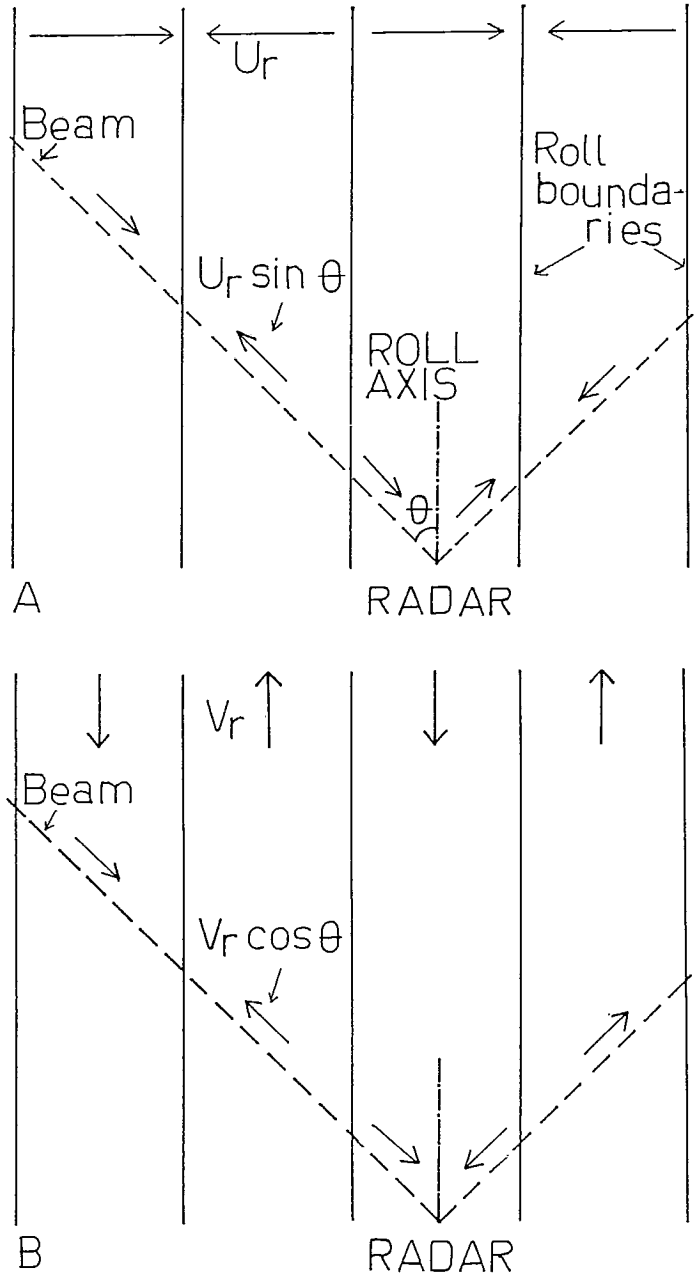

Fig. 3. Schematic picture showing the contributions of a) the cross-roll component *Ur* and b) the roll-parallel component *Vr* of the roll secondary circulation to the radial velocity pattern detected by a Doppler radar scanning in a plane roughly at the level of the lower part of the rolls.

Again, however, roll wavelength is the distance (measured perpendicular to the rolls) between two maxima (or minima) in the radial velocity.

In a real case both components *Ur* and *Vr* may contribute together. By comparing figs. 3a) and b) one can easily see that for rolls located to the left of the radar looking downwind the contributions of *Ur* and *Vr* are »in phase» thus increasing roll-to-roll differences in the radial velocity, while on the right hand side of the radar, the radial components of *Ur* and *Vr* partly compensate each other. In a real case, complications in the interpretation are caused by the typically unsymmetrical vertical structure of the rolls, the prevailing vertical wind profile and the height of the beam, typically increasing with range. On the other hand, by using elevation angles a little greater than 0 degrees, an estimate of the height of the roll circulation can also be obtained.

In order to study the appearance of various velocity patterns in the Doppler velocity scan, a simulation model has been developed (SAARIKIVI, 1986). The parameters that can be changed are

- the radar grid size and grid spacing,
- antenna elevation angle,
- PRF (The Nyqvist interval is divided into ten velocity ranges which depend on the PRF and wavelength),
- folding on/off.

The three-dimensional wind field is defined analytically. There are various built-in wind fields which may be selected by the user:

- constant *u*, *v*, and *w*,
- linear change in *u*, *v*, and *w*,
- horizontal or vertical discontinuity simulating a front,
- low-level jet,
- Ekman spiral,
- coastal convergence (the angle in the Ekman spiral may be different over the sea and the land),
- tornado,
- horizontal roll vortices.

In this study the model is used to simulate the effect of horizontal roll vortices on the Doppler velocity pattern. The Ekman spiral is added to the roll circulation. In the model the magnitude of the cross-roll and roll-parallel component of the wind, roll height and wavelength, and optional terminal fall-speed of scattering particles can be varied. In the Ekman spiral the magnitude of the geostrophic wind above the Ekman layer, the diffusion coefficient and the turning angle can be selected. As an example, the pure secondary roll circulation (*u* and *w* components of the wind) and the *v*-component of the wind in *x*–*z* plane is presented in fig. 4,

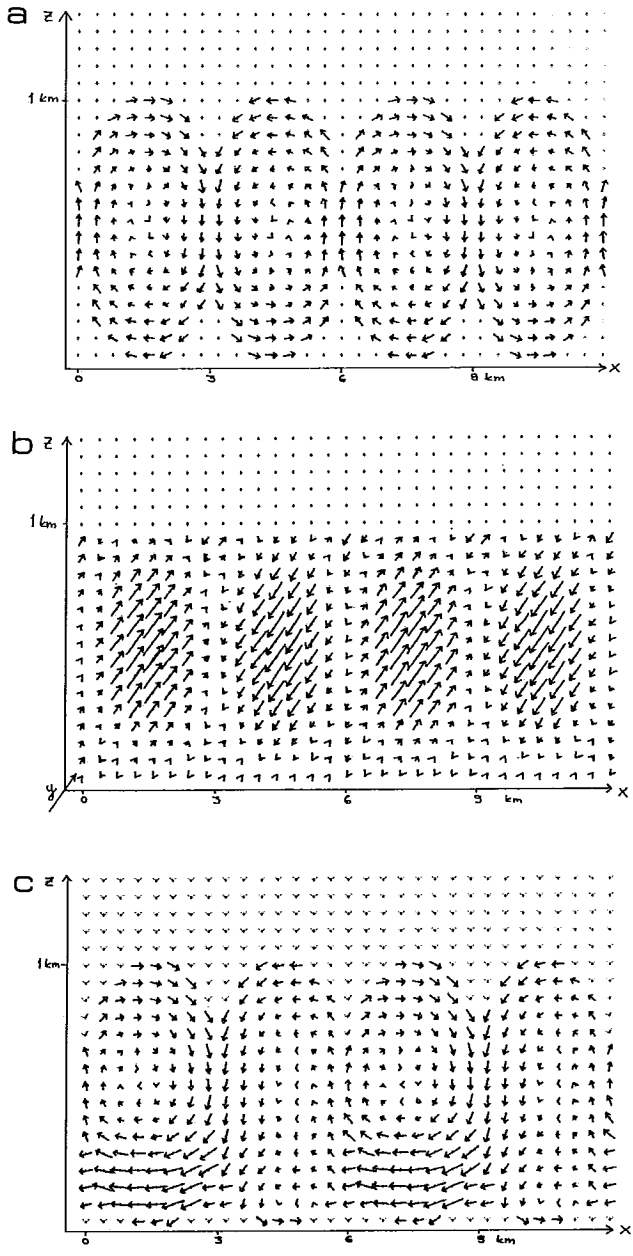

Fig. 4. a) The pure simulated roll circulation with constant basic flow in $x-z$ plane, b) the Vr-component of wind in $x-z$ plane. c) The roll circulation with the Ekman spiral flow added in $x-z$ plane.

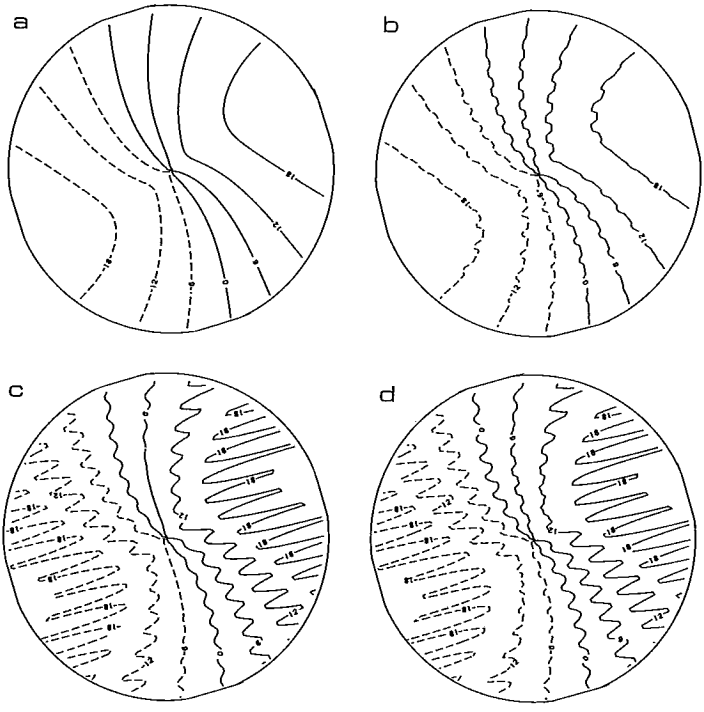

Fig. 5. Simulated radial Doppler velocity patterns for Jan. 29, 1985. Radar elevation angle 0.6 deg., radial velocities at 6 m/s intervals, maximum range displayed 50 km.
a) Pure Ekman profile. The angle between surface wind and geostrophic wind is 30 deg. The top of the Ekman layer is at 1 km where the wind speed is 20 m/s.
b) The Ekman profile of a) with rolls extending to 1 km and having a cross-roll component *Ur* of 1 m/s and wavelength of 6 km.
c) The Ekman profile of a) with a *Vr* component of ±4 m/s per 6 km in the x-direction in the Ekman layer.
d) The Ekman profile of a) combined with both *Ur* and *Vr* as in b) and c).

a) and b). The same field with the Ekman spiral added is shown in fig. 4, c).

Fig. 5 represents Doppler velocity simulations using those parameter values observed on Jan. 29, 1985. In all of the figures 5 a, b, c, and d, the prevailing wind profile is the same as shown alone in fig. 5a: an Ekman profile attaining just the observed wind velocity at the top of the PBL which was set to a height of 1 km. In fig. 5b only the cross-roll component *Ur* of the secondary circulation is added to the prevailing wind. Although as high a value as 1 m/s was used for *Ur* only a small effect can be observed in the radial velocity pattern. With the roll-parallel component *Vr* of the secondary circulation (but without *Ur*) as shown in fig. 5c, the secondary circulation can be observed more easily. In the simulation

Vr was assumed to be 20 % (± 4 m/s) of the wind at the top of the PBL. This may be a typical magnitude, according to model simulations by BROWN (1970) (see also fig. 2). Comparing figs. 5b and c with fig. 5d, where both *Ur* and *Vr* are present, it is seen that the contribution of *Vr* is clearly the major factor making horizontal rolls visible in a single Doppler radar measurement. Because *Vr* is not that component of the secondary circulation actually forming the rolls (as *Ur* does), one can never be absolutely sure that a saw-tooth pattern like fig. 5 really is an indication of a bona fide roll-circulation. It may also be caused, for example, by frictionally-induced lateral differences in the flow near a non-uniform ground. However, roll-like-circulations are most likely if »saw-tooth patterns» can be found not only at longer ranges up- and downstream from the radar, but also from beams pointing perpendicular to the assumed roll-axes close to the radar.

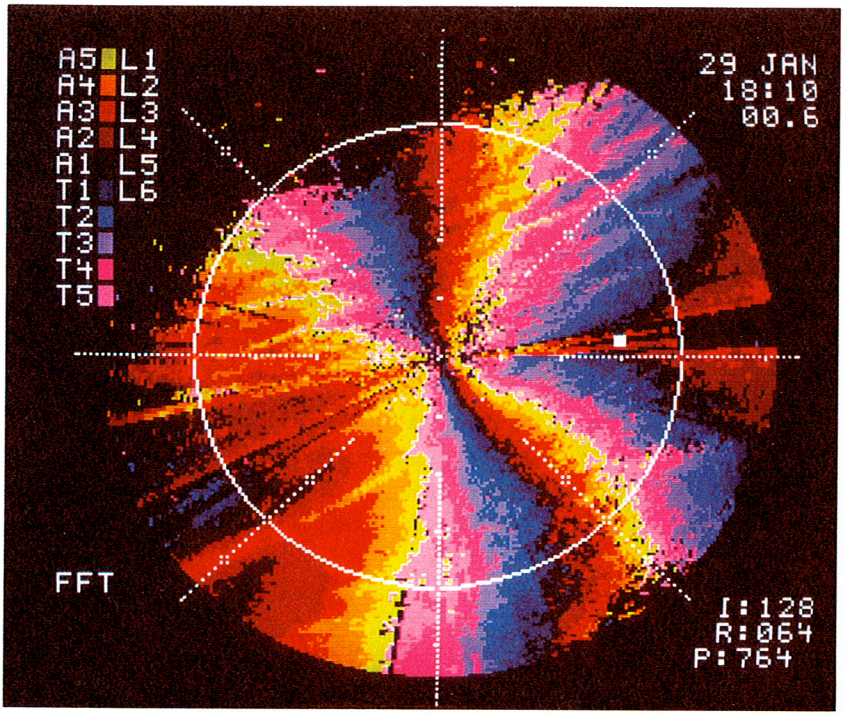

Fig. 6. The observed Doppler radial velocity pattern of Jan. 29, 1985 at 18.10 local time. Radar elevation angle is 0.6 deg. Unambiguous velocity range is ±10 m/s (PRF 764 Hz) and each colour represents a radial velocity interval of 2 m/s. Velocity scale is given in the upper left corner of the picture; *A*1 and *T*1 are the smallest radial velocities (0 to 2 m/s) away and towards the radar respectively and *A*5 and *T*5 are corresponding highest unambiguous (8 to 10 m/s) values. The maximum range displayed is 56 km.

If the flow pattern with rolls were homogeneous over the whole radar observing area the *Ur*-component could, in principle, be determined by observing differences across the rolls of the radial velocity on a radius which is perpendicular with the rolls. Similarly, the *Vr*-component of the secondary flow can then be determined by noting the roll-to-roll difference in the radial velocity at some distance from the radar in the direction of the roll axis and subtrating the (small) contribution of *Ur*. In fig. 5d the pure cross-roll component of the wind can be observed along the radii perpendicular with the rolls. The saw-tooth pattern showing up in the directions of the maximum and minimum velocities is mainly due to the roll-parallel component of the wind. The resemblance of the simulation to the observed pattern (fig. 6) is remarkable, in spite of the idealistic analytical representation of the roll circulation.

4. *Observations*

A very sensitive C-band Doppler weather radar WSR81C-D »Tuulia» located on the shoreline of the Gulf of Finland was used to observe horizontal roll vortices in the PBL. This radar is especially suitable for observing weak echoes and small velocity differences because a long pulse (2 μs) and a low PRF (250 Hz) could be selected for Doppler processing as well as for intensity estimation. The velocity resolution on colour displays was 0.66 m/s. For details of the radar system used, see PUHAKKA *et al.* (1986).

Radar measurements were not originally made with this study in mind. Thus the data are not complete and the most suitable for analysing roll circulations. However, altogether 20 radar observations from 9 roll cases, described in table 1, were included. Two of the cases were clear air situations, three were rolls within widespread rainfall and four within snowfall.

A velocity PPI-display was used to estimate the following parameters:

- Roll-orientation and wavelength.
- Variation in the radial velocity component across rolls (radial component of the secondary flow).
- Direction of the surface wind at the radar.
- Properties of the wind profile within the PBL (direction, speed, shear).
- Height of the roll circulation (could not be determined in all cases due to the lack of higher elevation data).

Figure 7 is an example of a radial velocity PPI picture obtained on Dec. 18, 1984. As shown with simulations in section 3, the main part of the radial component of the secondary flow arises from the variation of the roll-parallel wind

Table 1. Characteristics of roll cases studied. Legend: location L = land, S = sea; λ = wavelength; H = height; λ/H = aspect ratio; wind direction and roll orientation, degrees; roll intensity and wind speed, m/s; SST – TA = sea surface minus air temperature.

Day	Time and location		Radar estimated parameters					Weather and sea parameters		
			λ km	H km	λ/H	Surf.wind direction	Roll orient. & intens. Vr	850 mb wind	SST–TA	weather
84 Sep. 6	11.50	L	3	0.6	5	305	305/1.5	330/10	- 5	clear
–»–	12.30	L	4	0.6	6	305	305/1.5	330/10	- 5	–»–
–»–	16.30	L	10	2.2	5	305	305/2.0	330/10	- 5	–»–
Oct. 10	12.00	L	6	1.0	6	270	290/1.5	300/15	0	–»–
Sep. 10	15.30	L	6	–	–	150	150/3.0	180/18	- 1	rain
Sep. 25	12.15	L	3	0.5	6	90	90/3.0	120/18	0	–»–
Oct. 19	09.45	L	4	0.8	5	165	180/4.5	220/15	+ 1	–»–
–»–	–»–	S	3	0.5	6	165	180/1.5	220/15	+ 1	–»–
Nov. 23	10.45	L	2.5	0.8	3	135	155/1.5	160/20	+ 5	snow
–»–	12.20	L	5	0.8	6	120	125/1.5	160/20	+ 5	–»–
–»–	12.50	L	4	0.8	5	120	125/1.5	160/20	+ 5	–»–
–»–	17.50	L	4	0.8	5	120	130/2.5	160/20	+ 5	–»–
Dec. 17	09.00	L	4	0.7	6	120	120/2.5	120/20	+10	–»–
–»–	11.20	L	4	0.7	6	125	125/2.5	120/20	+10	–»–
–»–	13.30	L	7	0.7	10	130	130/2.0	120/20	+10	–»–
–»–	16.30	L	6	0.7	9	130	130/2.5	120/20	+10	–»–
Dec. 18	09.30	L	10	1.0	10	140	140/1.5	165/18	+ 9	–»–
–»–	–»–	S	5	0.5	10	140	140/1.0	165/18	+ 9	–»–
85 Jan. 29	17.10	L	6	1.0	6	235	250/3.0	265/12	–	–»–
–»–	18.20	L	6	1.0	6	235	250/4.0	265/12	–	–»–

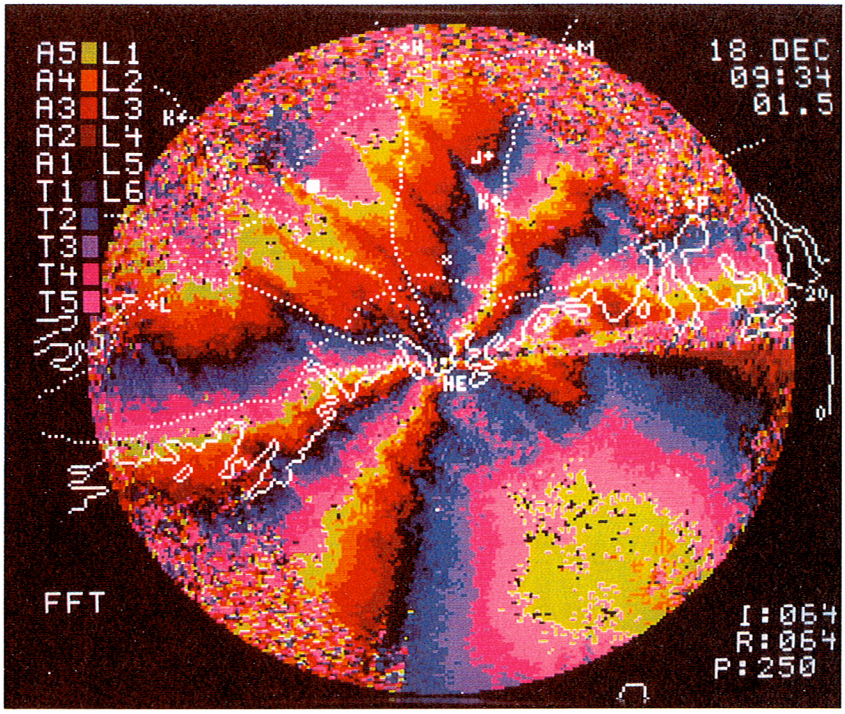

Fig. 7. Radial velocity PPI pattern of Dec. 18, 1984 at 9.34 local time. Radar elevation angle is 1.5 degrees, unambiguous velocity range ±3.3 m/s (PRF 250 Hz) and each colour represents a 0.66 m/s velocity interval. Maximum range displayed is 56 km.

in connection with rolls (component *Vr* in fig. 1), whereas the contribution of the cross-roll component, *Ur*, of the secondary flow may in most cases be almost negligible. In our example (fig. 7) *Ur* can hardly be detected, but *Vr* is very clear.

Roll heights were estimated as the heights where the saw-tooth-like radial velocity pattern disappeared. Such an estimate could be made for example from figures 7 and 8. As the data were not originally collected for this purpose, the height could not always be determined accurately because of the lack of a suitable elevation scan. The height of the capping inversion, if clearly defined in radiosonde soundings, was also used as an estimate of the roll height in some cases. In all cases studied, rolls could easily be identified from the Doppler velocity display but only in a few cases from the reflectivity display.

The mechanism causing echoes in rain and snowfall cases is obvious, but not

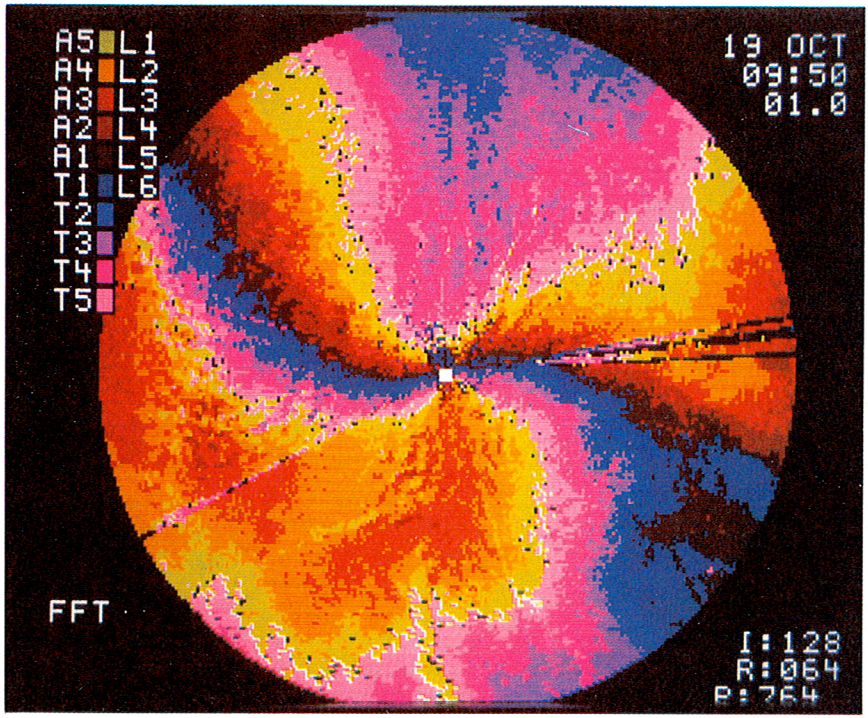

Fig. 8. Radial velocity pattern of Oct. 19, 1984 at 09.50 local time. Elevation angle is 1.0 deg. Other parameters as in Fig. 7.

much can be said of the origin of the clear air echoes. In another study (PUHAKKA *et al.*, 1986), we found, based on Doppler spectra, that birds were the main reason for a clear air sea-breeze echo. In the present study we made no observations of the Doppler spectra, but it seems very likely that biological targets of some kind (insects, seeds, birds?) may also have been responsible for echoes in the case of Sep. 6, 1984 (fig. 9). Refractive index fluctuations provide an alternative explanation, but because echoes were also observed over the relatively cool sea this may not be the main mechanism of scattering in this case.

Conventional weather observations made at Helsinki and Malmi Airports near the radar, and Jokioinen sounding station in Southern Finland and Tallin sounding station 80 km south of the radar were also used with synoptic weather analyses. Sea state (open/frozen) as well as sea surface temperatures were noted.

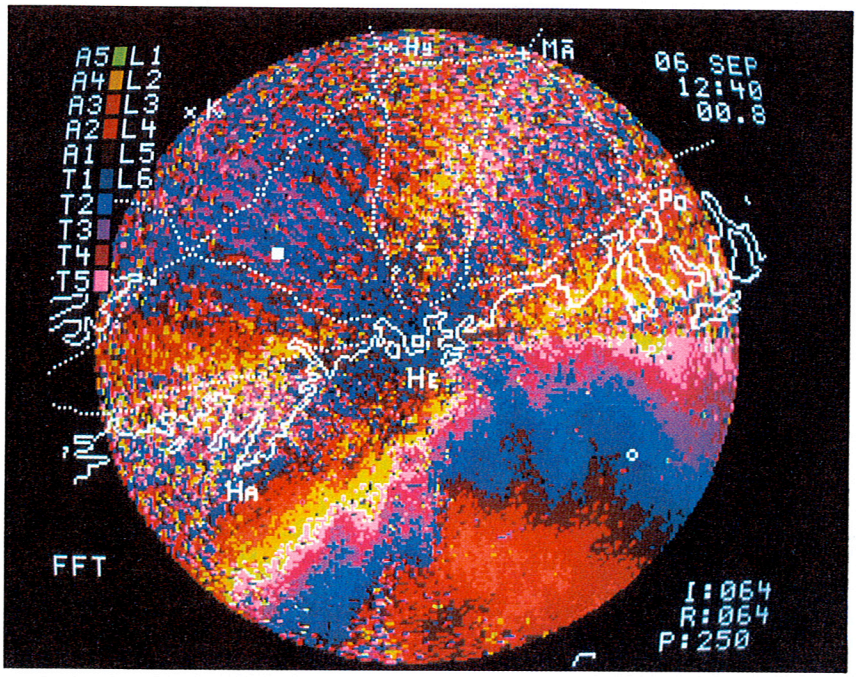

Fig. 9. An example of the radial velocity pattern in the »clear air» roll case of Sep. 6, 1984 at 12.40 local time. Elevation angle is 0.8 deg. Other parameters as in Fig. 8.

5. *Results*

The main result of our study is that PBL rolls frequently occur within frontal precipitation, in addition to the more commonly-reported »clear air» or cumulus-street cases. Of our 9 roll cases (table 1), 2 were clear-air situations, 3 were rainfall cases and 4 snowfall cases. All rainfall rolls occurred ahead of the warm surface front (or warmfront type of occlusion) while only one of the snowfall cases could be associated with a well-developed frontal system. All other roll-snowfall cases existed within scattered snowfall areas without any clear indication of a front. All 7 precipitating roll cases were fully cloudy. The typical parameters of precipitation rolls however, do not much differ from those reported so far. Roll wavelengths varied between 2.5 and 10 km and their aspect ratios between 3 and 10. The most common value of aspect ratio was 5 or 6.

In some cases roll wavelengths changed even during the observational period, but typically the aspect ratio remained nearly constant. A good example of this

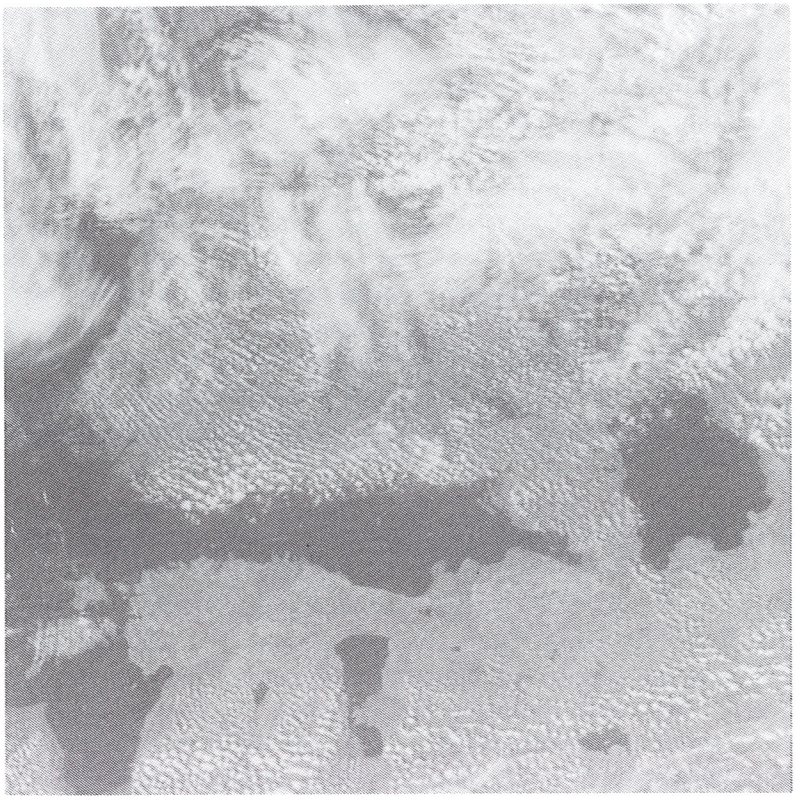

Fig. 10. Weather satellite picture for the »clear air» roll case (NOAA 7, Sep. 6, 1984 at 15.40 local time, Finnish Meteorological Institute). Cloud-streets cover Southern Finland, sea areas are cloudless.

is the clear air roll case of Sep. 6, 1984 (fig. 9, table 1). During the afternoon, roll wavelengths increased from about 3 km to 10 km, but as the depth of the PBL increased, according to the soundings from the same period, from 0.6 km to 2.2 km, the roll aspect ratio remained constant at a value of 5. A satellite picture (fig. 10) shows that the distances between the cumulus cloud streets, growing over the ascending parts of the rolls, also increased downstream indicating an increasing PBL depth. As can be seen from both radar and satellite pictures (figs. 9 and 10), rolls did not exist over the sea. This is easy to understand because the sea surface temperature was 5 degrees lower than the air temperature.

In all cases rolls were mainly observed over land areas. However, during two of the cases (Oct. 19, 1984 and Dec. 18, 1984) rolls were observed over both

land and sea simultaneously. As can be seen from figures 7 and 8, roll wavelengths and heights were in both cases smaller over the sea than over the land. As a result, the aspect ratio was again constant over both sea and land in each of the cases, being 5–6 in rainfall cases on Oct. 19, and as high as 10 in the snowfall case of Dec. 18. The reason for the big difference in the aspect ratios between these days is unknown. From table 1 one can see that in both cases the wind was from the Gulf of Finland and relatively strong, but in the rainfall case (with a smaller aspect ratio) the sea surface temperature was only slightly higher than the air temperature, while during the snowfall case the sea was about 9 degrees warmer than the air. For that reason the destabilizing effect of the advection of warm and moist air near the surface from the sea may have had an influence. This finding is in good agreement with the observations of KELLY (1984), who found that the »surface-layer-jump» over the sea was most strongly correlated with the aspect ratio.

In all roll cases the mean surface wind was 3.5 m/s or more (mean value 7 m/s), and the 850 mb wind was 8 m/s or more (mean 15 m/s). Orientation of the rolls was in most cases to the left of the 850 mb wind (up to 40 degrees) and up to 30 degrees to the right of the surface wind. In these cases directional shear varied between 50 and 70 degrees while in one case there was no directional shear. In all except that one case, the velocity profile was more or less »curved».

Typically, hydrostatic stability in the lowest layer was neutral or slightly unstable. A distinct capping inversion was found in only 6 of the 9 cases. In three of the snowfall cases, the sea surface temperature (*SST*) was more than 5 degrees Celsius higher than the air temperature, *TA*, (although rolls occurred mainly over the land). In one snowfall case the sea was frozen. In the rainfall cases and in one clear air case the *SST* was roughly the same as the air temperature. In the other clear air case, the *SST* was clearly lower than the *TA*.

According to the simulations in section 3, the intensity of roll circulation measurable by a single Doppler radar is mainly due to the variation of the roll-parallel component of the wind. Thus the differences in the radial component measured between individual rolls can be roughly interpreted as the *Vr* component of the secondary circulation. We measured values from ±1.0 m/s to ±4.5 m/s. If compared to the 850 mb wind these values are of the order of 5 up to 30 per cent of the 850 mb velocity, in very good agreement with earlier findings (BROWN (1970), LE MONE (1973)).

In order to make comparisons between roll cases and cases without rolls, 10 cases of radar data collected during snowfall but without any indication of PBL rolls, were also included in the analysis. It is clear that the small amount of data restricts the value of the comparisons. However, some differences found between

roll cases and no-roll cases may be important, In all roll cases the surface wind was higher than 3.5 m/s with a mean value of 7 m/s, while the corresponding mean surface wind was only 4 m/s in control cases. The same applies at the 850 mb level, where the mean wind speeds were 15 m/s and 9 m/s in roll and control cases, respectively. Another difference between roll and control cases, which may be significant, was that about 70 % of the roll cases had a slightly unstable PBL while the corresponding percentage was only 20 % for control cases. Thus the known fact that both moderate or strong winds and hydrostatic instability within the PBL are related to roll formation, seem also to be true in fully cloudy and precipitating roll cases.

6. *Concluding remarks*

Using observations from a single C-band Doppler weather radar, horizontal PBL roll vortices have been detected both in clear air and fully cloudy rain and snowfall cases. In all cases rolls existed over land, but only in two cases over the Gulf of Finland also. Otherwise the rolls were very similar to those observed earlier or predicted by model simulations.

In clear air and cumulus cases basic reasons for roll circulations are obvious: thermal convection caused by radiational warming of the surface together with moderate mean wind and vertical wind profile.

In rain and snowfall cases reasons for the roll formation are not as obvious, because radiational warming is prevented by fully cloudy skies. The following factors may be considered as potential reasons:

1. Frictionally-included low level convergence (rolls occurred mainly, and were most intensive, over the land, and in all cases the wind was from sea to land).
2. Frictionally-generated velocity profile which is more »curved» over the land than over the sea.
3. Low level potential instability caused by the advection of moist and relatively warm air from the sea over the land and released by the ascending motion caused by topography.

Acknowledgements: We wish to express our sincerest thanks to Anu Lahdensuu and Matti Leskinen for their help in collecting the data for this study.

REFERENCES

BERGER, M.I., and R.J. DOVIAK, 1979: *An analysis of the clear air planetary boundary layer wind synthesized from NSSL's dual Doppler-radar data.* NOAA-ERL-NSSL-87, National Severe Storms Laboratory, Norman, OK, 55 pp.

BROWN, R.A., 1970: A secondary flow model for the planetary boundary layer. *J. Atmos. Sci.*, 27, 742–757.

–»– , 1980: Longitudinal instabilities and secondary flows in the planetary boundary layer: a review. *Rev. Geophys. Space Phys.*, 18, 683–697.

BRÜMMER, B., 1985: Structure, dynamics and energetics of boundary layer rolls from Kontur aircraft observations. *Beitr. Phys. Atmosph.*, 58, 237–254.

FALLER, A.J., and R.E. KAYLOR, 1966: A numerical study of the instability of the laminar Ekman boundary layer. *J. Atmos. Sci.*, 23, 466–480.

HILDEBRAND, P.H., 1980: Multiple Doppler radar observations of PBL structure. *Preprints 19th Conf. on Radar Meteorology, Miami Beach, Amer. Meteor. Soc.*, 656–661.

KELLY, R.D., 1982: A single Doppler radar study of horizontal roll convection in a lake-effect snow storm. *J. Atmos. Sci.*, 39, 1521–1531.

–»– , 1984: Horizontal roll and boundary-layer interrelationships observed over Lake Michigan. *Ibid.*, 41, 1816–1826.

KONRAD, T.G., 1968: The alignment of clear-air convective cells. *Preprints Int. Conf. on Cloud Physics, Toronto, Amer. Meteor. Soc.*, 539–543.

KROPFLI, R.A., and N.M. KOHN, 1978: Persistent horizontal rolls in the urban mixing layer as revealed by dual-Doppler radar. *J. Appl. Meteor.*, 17, 669–676.

KUETTNER, J.P., 1959: The band structure of the atmosphere. *Tellus*, 11, 267–294.

–»– , 1971: Cloud bands in the earth's atmosphere: Observations and theory. *Ibid.*, 23, 404–425.

LEMONE, M.A., 1973: The structure and dynamics of horizontal roll vortices in the planetary boundary layer. *J. Atmos. Sci.*, 30, 1077–1091.

–»– , 1976: Modulation of turbulence energy by longitudinal rolls in an unstable planetary boundary layer. *Ibid.*, 33, 1308–1320.

MASON, P.J., 1985: A numerical study of cloud streets in the planetary boundary layer. *Boundary Layer Met.*, 32, 281–304.

MÜLLER, D., ETLING, D., KOTTMEIER, Ch., and R. ROTH, 1985: On the occurrence of cloud streets over northern Germany. *Quart. J. R. Met. Soc.*, 111, 761–772.

PUHAKKA, T., KOISTINEN, J., and P. SMITH, 1986: Doppler radar observation of a sea-breeze front. *Preprints, 23rd Conf. on Weather Radar, Amer. Meteor. Soc., Boston, Mass.*, 4 pp.

RABIN, R.M., DOVIAK, R.J., and A. SUNDARA-RAJAN, 1981: Doppler radar observations of momentum flux in cloudless convective layer with rolls. *J. Atmos. Sci.*, 39, 851–863.

SAARIKIVI, P., 1986: Simulation model of a single Doppler radar velocity patterns. To be published in: *University of Helsinki, Department of Meteorology, Report series.*